Terahertz Laser with Optically Pumped Graphene Layers and Fabri–Perot Resonator

Terahertz Laser with Optically Pumped Graphene Layers and Fabri–Perot Resonator

Alexander A. Dubinov[1,2], Vladimir Ya. Aleshkin[2], Maxim Ryzhii[1,3], Taiichi Otsuji[3,4], and Victor Ryzhii[1,3]

[1] *Computational Nanoelectronics Laboratory, University of Aizu, Aizu-Wakamatsu, Fukushima 965-8580, Japan*
[2] *Institute for Physics of Microstructures, Russian Academy of Sciences, Nizhny Novgorod 603950, Russia*
[3] *Japan Science and Technology Agency, CREST, Chiyoda, Tokyo 107-0075, Japan*
[4] *Research Institute for Electrical Communication, Tohoku University, Sendai 980-8577, Japan*

Received June 10, 2009; accepted July 21, 2009; published online August 21, 2009

We propose and substantiate the concept of terahertz (THz) laser based on the optically pumped graphene layers and the resonant cavity of the Fabri–Perot type. The pumping scheme which corresponds to the optical interband excitation of graphene followed by the emission of an optical phonons cascade provides the population inversion for the interband transitions in a relatively wide range of THz frequencies. We demonstrate that the THz lasing in the device under consideration at room temperatures is feasible if its structure is optimized. The frequency and output power of the generated THz radiation can be tuned by varying the distance between the mirrors.

DOI: 10.1143/APEX.2.092301

Recent experimental and theoretical studies have demonstrated that graphene layers and their stacks exhibit unusual electron and optical properties, that may be used in the design of novel electron and optoelectron devices.[1–3] Under optical excitation, the interband population inversion in graphene can be achieved.[4–6] Due to the gapless energy spectrum of graphene, such a population inversion can lead to the stimulated emission of long-wavelength photons, in particular, the photons in the terahertz (THz) range of frequencies. The results of recent experiments[7] confirm this. In this paper, we propose the concept of a THz laser based on an optically pumped graphene heterostructure (GHS) with a Fabri–Perot type resonator and substantiate this concept.

The active section of the laser proposed consists of a pure separating Si layer of thickness t followed by a graphene–SiC–Si–SiC–graphene GHS (with thin SiC layers) of the net thickness d. Thus, the laser active section comprises two separated graphene layers. The first (separating) Si layer is adjacent to a metal mirror (made of, say, Al, Au, or Ag). Another mirror with an output hole of diameter $2a$ is placed at the distance L from the first one, so that a Fabri–Perot resonator (with the diameter $2R$) is formed. The laser structure in question is shown in Fig. 1(a). Slightly different laser with a suspended GHS, i.e., the GHS separated from the mirror by an air layer (with thickness $t_{\rm air}$), shown in Fig. 1(b), is also considered. The graphene layers are excited by optical radiation with the photon energy $\hbar\Omega$ [as shown schematically in Fig. 1(b)]. It is assumed that $\hbar\Omega$ somewhat exceeds the value $2n\hbar\omega_0 = \hbar\Omega_0$, namely, $\hbar\Omega \gtrsim \hbar\Omega_0 + \varepsilon_{\rm F}$, where $\hbar\omega_0 \simeq 0.2\,{\rm eV}$ is the optical phonon energy, $n = 1, 2, \ldots$, and $\varepsilon_{\rm F}$ is the electron and hole quasi-Fermi energy. In this case, as predicted theoretically[4–6] and investigated experimentally (for instance, in refs. 7–9), the photogeneration of electrons and holes followed by the emission of an optical phonon cascade, results in substantial electron and hole populations of the conduction band bottom and the valence band top, respectively, [see Figs. 1(c) and 1(d)].

The dynamic ac conductivity of an optically pumped graphene layer σ_ω comprises both the interband and intraband contributions, so that

$$\mathrm{Re}\,\sigma_\omega = \mathrm{Re}\,\sigma_\omega^{(\rm inter)} + \mathrm{Re}\,\sigma_\omega^{(\rm intra)}. \tag{1}$$

If the electron and hole energy distributions near the band edges are characterized by the Fermi distribution functions

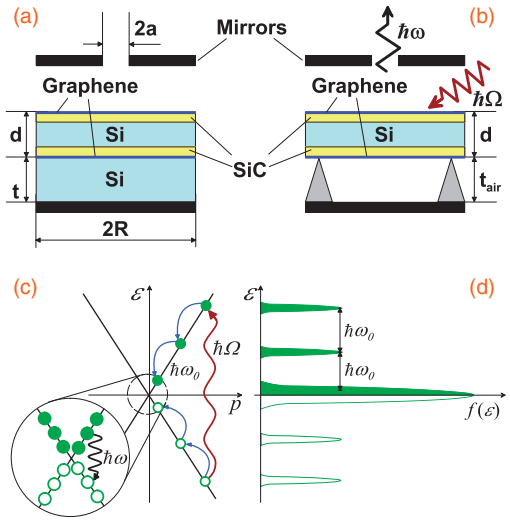

Fig. 1. Schematic view of the laser structures with Si separation layer (a) and with air separation layer (b), as well as the laser pumping scheme (c) and electron and hole distribution functions (d). Tooth-like arrows on panel (b) indicate the directions of optical pumping radiation and output THz radiation with the photon energies $\hbar\Omega$ and $\hbar\omega$, respectively. Arrows on panel (c) correspond to the pertinent transitions.

with the quasi-Fermi energy $\varepsilon_{\rm F}$ and the effective temperature T, one obtains (for the ac electric field directed in the graphene plane)

$$\mathrm{Re}\,\sigma_\omega^{(\rm inter)} = \frac{e^2}{4\hbar}\tanh\left(\frac{\hbar\omega - 2\varepsilon_{\rm F}}{4k_{\rm B}T}\right), \tag{2}$$

$$\mathrm{Re}\,\sigma_\omega^{(\rm intra)} = \frac{2e^2k_{\rm B}T\tau\ln[1+\exp(\varepsilon_{\rm F}/k_{\rm B}T)]}{\pi\hbar^2(1+\omega^2\tau^2)}. \tag{3}$$

Here e is the electron charge, $k_{\rm B}$ is the Boltzmann constant, and τ is the electron and hole momentum relaxation time (which is assumed independent on the energy). The case $\varepsilon_{\rm F} = 0$ corresponds to the equilibrium, while the case $\varepsilon_{\rm F} > 0$ corresponds to the interband population inversion. As follows from eq. (3) in the latter case, $\mathrm{Re}\,\sigma_\omega^{(\rm inter)} < 0$ for $\hbar\omega < 2\varepsilon_{\rm F}$. Since the electron and hole densities increase with increasing optical pumping intensity I_Ω, the quasi-Fermi energy $\varepsilon_{\rm F}$ also increases. This implies that at sufficiently strong pumping, $\mathrm{Re}\,\sigma_\omega$ can become negative in a certain range of frequencies. Equations for $\mathrm{Re}\,\sigma_\omega^{(\rm inter)}$ and $\mathrm{Re}\,\sigma_\omega^{(\rm intra)}$ were obtained for the Fermi distributions of electrons and holes near the edge of the bands. If the electron–electron, electron–hole, and hole–hole

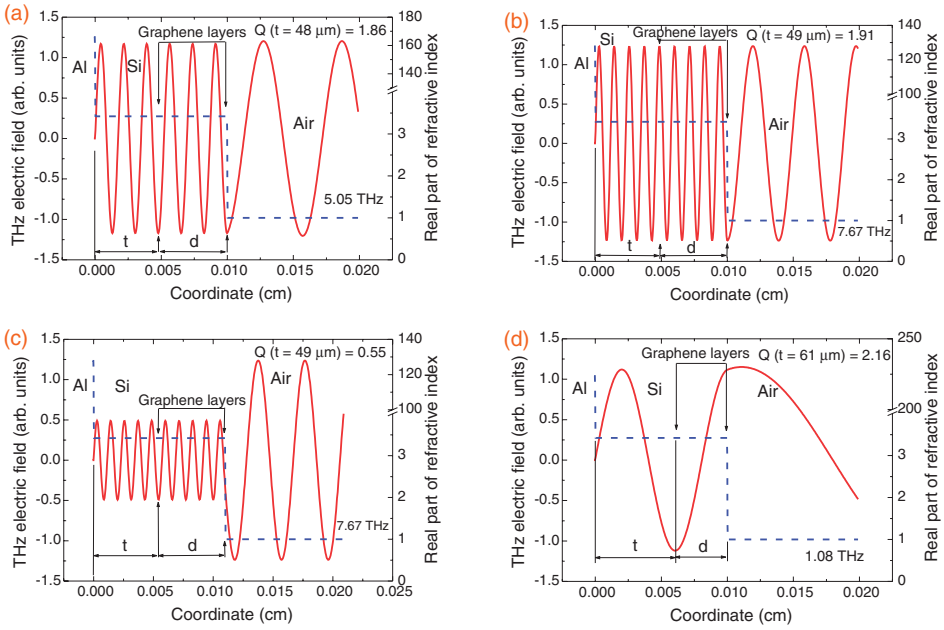

Fig. 2. Spatial distributions of THz electric field (red lines) and real part of refractive index (blue lines).

interactions do not provide an effective "fermisation" of the electron and hole energy distributions in a narrow energy range near $\varepsilon = 0$, the equations in question should be modified taking into account the deviation of the distributions from the Fermi distribution.[5)]

To determine the conditions of lasing for the lasers with different structural parameters, we introduce the efficiency coefficient Q, which is the ratio of the THz radiation (polarized in the graphene layer plane) power generated in the graphene layers to the THz power absorbed in the mirrors and Si-layers:

$$Q = \frac{(8\pi/c)\,\mathrm{Re}\,\sigma_\omega[E^2|_{z=t} + E^2|_{z=t+d}]}{(1-r_1)E_1^2 + (1-r_2)E_2^2 + (a/R)^2E_1^2 + E_{\mathrm{Si}}^2} \quad (4)$$

with

$$E_{\mathrm{Si}}^2 = (\alpha_{\mathrm{Si}}\, n_{\mathrm{Si}}/2)\int_0^{t+d} E^2\, dz.$$

Here $E = E(z)$ is the amplitude of the THz electric field, E_1 and E_2 are the maximum amplitudes of the THz electric field in the space between the first mirror and the nearest graphene layer and the second mirror and the graphene layer nearest to the latter, respectively, r_1 and r_2 are the reflection coefficients from metal mirrors, α_{Si} and n_{Si} are the absorption coefficient and real part of the refraction index of Si, and c is the speed of light. The third and fourth terms in the denominator in eq. (4) correspond to the losses of THz radiation due to its output through the hole in the second mirror and to the absorption in the Si layers. In the case of the laser structure shown in Fig. 1(b),

$$E_{\mathrm{Si}}^2 = (\alpha_{\mathrm{Si}}\, n_{\mathrm{Si}}/2)\int_{t_{\mathrm{air}}}^{t_{\mathrm{air}}+d} E^2\, dz.$$

The absorption of THz radiation in fairly thin SiC layers is neglected. The diffraction losses are also disregarded due to $\lambda = 2\pi c/\omega < a \ll R$. The condition $Q > 1$ corresponds to the THz lasing.

The spatial distributions of the THz electric field inside the Fabri–Perot resonator was calculated using the Maxwell equations considering the features of the layers. It was assumed that the electron and hole quasi-Fermi energies in graphene layers under optical pumping are $\varepsilon_{\mathrm{F}} = 60\,\mathrm{meV}$ and the mobility is[10)] $\mu = 200{,}000\,\mathrm{cm}^2/(\mathrm{V{\cdot}s})$ at the temperature $T = 300\,\mathrm{K}$ ($\tau = 1\,\mathrm{ps}$). As follows from eqs. (2) and (3), this corresponds to $\sigma_\omega = -5.76 \times 10^7\,\mathrm{cm/s}$ at $f = \omega/2\pi = 5.05\,\mathrm{THz}$ ($\hbar\omega = 20.88\,\mathrm{meV}$), so that $2\hbar|\sigma_\omega|/e^2 = 0.50$. We set $a/R = 0.1$ and $r_1 = r_2 = 0.99$. The data for the characteristics of Si and metal mirrors (Al) in the range of the frequencies under consideration were taken from ref. 11. The calculated spatial distributions of the THz electric field are demonstrated in Fig. 2. In particular, the plot in Fig. 2(a) corresponds to $t = 48\,\mu\mathrm{m}$ and $d = 52\,\mu\mathrm{m}$ (so that $t + d = 100\,\mu\mathrm{m}$). For the distribution shown in Fig. 2(a), using eq. (4), one obtains $Q = 1.86$ (i.e., $Q > 1$). However, at $t = 43\,\mu\mathrm{m}$ and $d = 57\,\mu\mathrm{m}$, Q reaches a minimum: $Q = 0.95$. For the frequency $f = 7.67\,\mathrm{THz}$ (31.72 meV) for which $\sigma_\omega = -6.55 \times 10^7\,\mathrm{cm/s}$ with $2\hbar|\sigma_\omega|/e^2 \simeq 0.57$, at $t = 49\,\mu\mathrm{m}$ and $d = 51\,\mu\mathrm{m}$ [see Fig. 2(b)], as well as at $t = 46\,\mu\mathrm{m}$ and $d = 54\,\mu\mathrm{m}$, our calculations yield $Q = 1.91$ and 1.01, respectively. In all the above cases, the net thickness was assumed to be $t + d = 100\,\mu\mathrm{m}$. If the latter value varies, the spatial distribution of the THz electric field can change dramatically. Indeed, for $f = 7.67\,\mathrm{THz}$, setting $t = 49\,\mu\mathrm{m}$ and $d = 61\,\mu\mathrm{m}$, so that $t + d = 110\,\mu\mathrm{m}$, one obtains the distribution shown in Fig. 2(c) with $Q = 0.55$. At $t = 46\,\mu\mathrm{m}$ and $d = 64\,\mu\mathrm{m}$, the value of Q becomes rather small: $Q = 0.2$. This implies that the fulfillment of the condition of the THz lasing $Q > 1$ in the laser structures under consideration with two graphene layers is real but it requires a careful optimization of the graphene structure (proper choice of the thicknesses of the Si layers and the spacing between the mirrors). Figure 2(d) shows the spatial distribution of the THz electric field calculated for a laser with the frequency $f = 1.08\,\mathrm{THz}$ ($\hbar\omega = 4.48\,\mathrm{meV}$). It is assumed that $t = 61\,\mu\mathrm{m}$, $d = 39\,\mu\mathrm{m}$, and the pumping corresponds to $\varepsilon_{\mathrm{F}} = 17\,\mathrm{meV}$ at $T = 77\,\mathrm{K}$. This provides $\sigma_\omega = -5 \times 10^7\,\mathrm{cm/s}$ with $2\hbar|\sigma_\omega|/e^2 \simeq 0.43$. The obtained

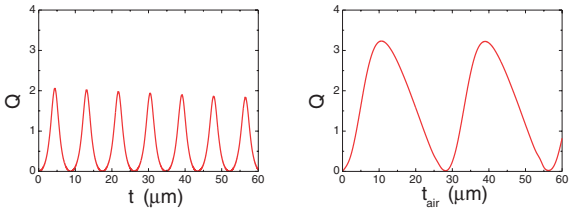

Fig. 3. Coefficient of efficiency Q as a function of Si separation layer thickness t (a) and air separation layer thickness t_{air} (b).

value of the efficiency coefficient is $Q = 2.16$.

The frequency dependence of σ_ω is associated with the following two factors: a temperature smearing of the Fermi distribution and a weakening of the Drude absorption with increasing frequency (the Drude absorption decreases with increasing mobility). This is why the transfer to the low end of the THz range requires a decrease in the temperature or an increase in the mobility.

Figure 3(a) shows the dependence of coefficient Q on the separating Si layer thickness t for a laser with $L = 1$ cm and $d = 52\,\mu$m for $f = 5.05$ THz (20.88 meV). One can see that Q as a function of t varies quasiperiodically with the period $\lambda/2n_{Si}$, where $\lambda = 59.4\,\mu$m is the wave length in vacuum (air). A decrease in the amplitude of oscillations is associated with an increase in absorption of THz radiation in the separating Si layer when its thickness t increases. In the laser with the suspended GHS [see Fig. 1(b)], in which the absorption of TH radiation between the GHS and the mirrors can be neglected, the Q versus t_{air} dependence exhibits a larger amplitude and it is purely periodic. Such a dependence is shown in Fig. 3(b) for $d = 50\,\mu$m and $f = 5.3$ THz (21.9 meV). The efficiency coefficient Q exhibits similar oscillations as a function of the spacing between the mirrors L. Hence, varying L, one can mechanically tune the frequency of THz radiation and the output THz power.

The lasing in the devices under consideration can also be achieved if the graphene layers are less perfect than it was assumed above, exhibiting rather modest mobility. However, in such a case, lower temperatures might be required and the generation of radiation with elevated frequency can merely be possible. The former is associated with the necessity to increase the intensity of the interband transitions by suppressing the temperature smearing of the electron and hole distributions to compensate an increase in the Drude absorption with decreasing mobility and, hence, decreasing momentum relaxation time τ. The frequency shift can be attributed to the fact that the Drude absorption is proportional to $1/\omega^2\tau$. Hence, a decrease in the momentum relaxation time τ can be compensated by an increase in the frequency ω. Our calculations show that even at electron (hole) mobility $\mu = 20{,}000\,\mathrm{cm^2/(V{\cdot}s)}$,[12] the lasing in the THz frequency range is possible at $T = 77$ K. At room temperatures (RTs), the lasing using "low quality" GHS can also be realized but in the mid-infrared range.

The threshold optical power density S_Ω^{th} depends on the required value of the quasi-Fermi energy ε_F (and, hence, the electron and hole density Σ) and the recombination time τ_R. The mechanisms determining the latter are not well understood yet. Considering the experimental date[7] (see also ref. 8), we set $\tau_R = 10$ ps and, hoping that the recombination time can be increased in GHS with weaker disorder, $\tau_R = 100$ ps. We estimate S_Ω^{th} (as in ref. 4) using eqs. (2) and (3) in which the Fermi energy ε_F is determined by the electron and hole densities. Assuming $\hbar\Omega = 920$ meV and $\varepsilon_F = 60$ meV ($n = 2$), we obtain $\Sigma \simeq 3 \times 10^{11}\,\mathrm{cm^{-2}}$ and $S_\Omega^{th} \simeq 5 \times (10^3$–$10^4)\,\mathrm{W/cm^2}$ [with the absorbed power density $S_\Omega^{*th} \simeq 5 \times (10^2$–$10^3)\,\mathrm{W/cm^2}$]. At $\hbar\Omega = 120$ meV (CO_2 laser) and $\varepsilon_F \lesssim 60$ meV, one obtains $S_\Omega^{th} \simeq 6.5 \times (10^2$–$10^3)\,\mathrm{W/cm^2}$. If $\varepsilon_F = 20$ meV, the required optical power is $S_\Omega^{th} \simeq 5 \times (10^2$–$10^3)\,\mathrm{W/cm^2}$. The mirrors can also serve as a resonator for input optical radiation. In this case, the input pumping power can be reduced by the value of the optical resonator quality factor $Q_\Omega \gg 1$. Assuming that the stimulated radiative recombination surpasses the nonradiative recombination (the pumping optical power density S_Ω markedly exceeds the threshold value S_Ω^{th}) and taking into account that the pumping optical radiations crosses GHS twice, one can obtain the following rough estimate for the output THz power: $P_\omega = K\,(\pi R^2)S_\Omega$, where $K = (4\pi e^2/\hbar c)(\omega/\Omega)$. In the case of pumping by a CO_2 laser and $\omega/\Omega \simeq 1/6$, $K \simeq 1.6\%$. If $2R = 0.1$ cm and $S_\Omega = 10^4\,\mathrm{W/cm^2}$, one obtains $P_\omega \simeq 1.25$ W.

One needs to point out that the energy of optical radiation photons $\hbar\Omega$ should be chosen to provide sufficiently small value $\hbar\Omega - \hbar\Omega_0 - \varepsilon_F$. Otherwise, the excessive energy of the photogenerated electrons and holes (after the emission of the optical phonon cascade) might result in a marked heating of the electron–hole system[13] and shortening of the recombination time due to the inclusion of the recombination associated with the emission of optical phonons[14] The latter can prevent the achievement of THz lasing.

In conclusion, we proposed a tunable THz laser based on optically pumped GHS placed in the Fabri–Perot resonator and demonstrated the feasibility of its operation at RT.

Acknowledgment This work was supported by the Japan Science and Technology Agency, CREST, Japan. A. A. Dubinov and V. Ya. Aleshkin also acknowledge the support by the Russian Academy of Sciences, Russia.

1) C. Berger, Z. Song, T. Li, X. Li, A. Y. Ogbazhi, R. Feng, Z. Dai, A. N. Marchenkov, E. H. Conrad, P. N. First, and W. A. de Heer: J. Phys. Chem. **108** (2004) 19912.
2) K. S. Novoselov, A. K. Geim, S. V. Morozov, D. Jiang, M. I. Katsnelson, I. V. Grigorieva, S. V. Dubonos, and A. A. Firsov: Nature **438** (2005) 197.
3) A. K. Geim and K. S. Novoselov: Nat. Mater. **6** (2007) 183.
4) V. Ryzhii, M. Ryzhii, and T. Otsuji: J. Appl. Phys. **101** (2007) 083114.
5) A. Satou, F. T. Vasko, and V. Ryzhii: Phys. Rev. B **78** (2008) 115431.
6) V. Ya. Aleshkin, A. A. Dubinov, and V. Ryzhii: JETP Lett. **89** (2009) 63.
7) T. Otsuji, Y. Tsuda, H. Karasawa, T. Suemitsu, M. Suemitsu, E. Sano, and V. Ryzhii: Proc. 17th Int. Symp. Nanostructures: Physics and Technology, Minsk, June 22–27, 2009.
8) D. Sun, Z.-K. Wu, C. Divin, X. Li, C. Berger, W. A. deHeer, P. N. First, and T. B. Norris: Phys. Rev. Lett. **101** (2008) 157402.
9) J. M. Dawlaty, S. Shivaraman, M. Chandrashekhar, F. Rana, and M. G. Spencer: Appl. Phys. Lett. **92** (2008) 042116.
10) S. V. Morozov, K. S. Novoselov, M. I. Katsnelson, F. Schedin, D. C. Elias, J. A. Jaszczak, and A. K. Geim: Phys. Rev. Lett. **100** (2008) 016602.
11) E. D. Palik: *Handbook of Optical Constants of Solids* (Academic Press, New York, 1998) p. 192.
12) Y.-W. Tan, Y. Zhang, K. Bolotin, Y. Zhao, S. Adam, E. H. Hwang, S. Das Sarma, H. L. Stormer, and P. Kim: Phys. Rev. Lett. **99** (2007) 246803.
13) V. Ryzhii, M. Ryzhii, and T. Otsuji: Phys. Status Solidi C **5** (2008) 261.
14) F. Rana, P. A. George, J. H. Strait, J. Dawlaty, S. Shivaraman, M. Chandrashekhar, and M. G. Spencer: Phys. Rev. B **79** (2009) 115447.